



## Development of Proton Conducting Ceramic Cells in Metal Supported Architecture

Noriko Sata<sup>1</sup> , Feng Han<sup>1</sup> , Haoyu Zheng<sup>1</sup>, Amir Masoud Dayaghi<sup>2</sup>, Truls Norby<sup>2</sup>, Marit Stange<sup>3</sup>, Robert Semerad<sup>4</sup> and Rémi Costa<sup>1</sup>

© 2021 ECS - The Electrochemical Society

[ECS Transactions](#), [Volume 103](#), [Number 1](#)

**Citation** Noriko Sata *et al* 2021 *ECS Trans.* **103** 1779

**DOI** 10.1149/10301.1779ecst

---

[+ Article and author information](#)

### Abstract

Metal-Supported (MS) architecture offers various advantages over state-of-the-art ceramic supported SOCs, such as high tolerance towards thermal/redox cycling that are key features for flexible and reliable operation in high temperature fuel cell and electrolysis applications. Our target is to develop Proton-conducting Ceramic Cells (PCC) in MS architecture, of which combination can provide potentially high performances, mechanical stability, and flexibility for wide range of electrochemical applications. The key challenge in the development of MS-PCC is to find a feasible process to fabricate gas-tight electrolyte on the porous metal substrate without degrading the metal support and the electrolyte. Our strategy is implementing multilayers combining wet chemical processes below 1000°C for the functional electrode and dry Physical Vapor Deposition (PVD) techniques below 800°C for the gas-tight electrolyte coating. In this paper, we present our recent results in the development of MS-PCC half cells. The materials selection for MS and PCC components, functional layer processing, and electrolyte layer deposition techniques are discussed.

Export citation and abstract

[BibTeX](#)

[RIS](#)

# Development of Proton Conducting Ceramic Cells in Metal Supported Architecture

N. Sata<sup>a</sup>, F. Han<sup>a</sup>, H. Zheng<sup>a</sup>, A. M. Dayaghi<sup>b</sup>, T. Norby<sup>b</sup>, M. Stange<sup>c</sup>, R. Semerad<sup>d</sup>,  
and R. Costa<sup>a</sup>

<sup>a</sup> German Aerospace Center (DLR), Pfaffenwaldring 38-40, D-70569 Stuttgart, Germany

<sup>b</sup> Centre for Materials Science and Nanotechnology, University of Oslo, Norway

<sup>c</sup> SINTEF, Forskningsveien 1, NO-0373 Oslo, Norway

<sup>d</sup> Ceraco Ceramic Coating GmbH, Rote-Kreuz-Str. 8, D-85737 Ismaning, Germany

Metal-Supported (MS) architecture offers various advantages over state-of-the-art ceramic supported SOCs, such as high tolerance towards thermal/redox cycling that are key features for flexible and reliable operation in high temperature fuel cell and electrolysis applications. Our target is to develop Proton-conducting Ceramic Cells (PCC) in MS architecture, of which combination can provide potentially high performances, mechanical stability and flexibility for wide range of electrochemical applications. The key challenge in the development of MS-PCC is to find a feasible process to fabricate gas-tight electrolyte on the porous metal substrate without degrading the metal support and the electrolyte. Our strategy is implementing multilayers combining wet chemical processes below 1000°C for the functional electrode and dry Physical Vapor Deposition (PVD) techniques below 800 °C for the gas-tight electrolyte coating. In this paper, we present our recent results in the development of MS-PCC half cells. The materials selection for MS and PCC components, functional layer processing and electrolyte layer deposition techniques are discussed.

## Introduction

Increasing demand for hydrogen energy and interest for P2X applications has accelerated research and development of Solid Oxide Cells (SOC) in a wide range of technologies and applications. In fuel-cell and electrolysis applications, reliability, long-term stability, lower cost as well as high performance are essential. Metal-Supported (MS) architecture offers various advantages over state-of-the-art ceramic supported SOCs, such as high tolerance towards thermal/redox cycling that are key features for flexible and reliable operation. MS-SOC has been studied in fuel-cell (1) and electrolysis applications (2), and an exceptionally high power density of MS-SOC in fuel cell operation has been achieved up to 2.8 A cm<sup>-2</sup> at 650°C and 0.7 V (3). One of the drawbacks of MS-SOC in fuel cell and electrolysis application is the corrosive environment due to steam in fuel electrode, i.e. on the metal support that could cause degradation of the metal substrate. High temperature Proton Conducting Ceramic (PCC) materials have been intensively studied and demonstrated promising improvements in the last decade. Different in geometric layout from SOC in terms of steam production in fuel cells and steam supply in electrolysis cells, PCC is advantageous for its low oxygen partial pressure in fuel electrode compartment, not merely to optimize the electrochemical operation, but also to mitigate the risk of metal support

corrosion in MS architecture. The challenge in the development of MS-PCC is to find a feasible process to fabricate gas-tight electrolyte on the porous substrate without degrading the metal support and the electrolyte materials. The state-of-the-art PCC electrolyte is based on perovskite oxides that have refractory nature requesting high sintering temperature typically above 1400 °C, which makes it more challenging for MS-PCC than for MS-SOC via sintering method.

The paper presents our recent activities in the development of MS-PCC aiming at the development of a common technological platform in the form of planar half cells for different applications. This includes steam electrolysis application and hydrogen pumping. In project DAICHI (2018-2022, [www.dlr.de/tt/DAICHI](http://www.dlr.de/tt/DAICHI), EIG-CONCERT-Japan), where we started MS-PCC development for steam electrolysis application, the concept of the architecture was demonstrated by the cell structure with about 1 µm-thick electrolyte of reasonable proton conductivity. The concept is further developed with a more cost effective design and scalable techniques in the project ARCADE (2019-2023, BMBF). In project 112CO2 (2020-2024, [www.112co2.eu](http://www.112co2.eu), Horizon 2020), the target application of MS-PCC is hydrogen pumping from the reactor, i.e. both electrodes working under reducing condition, that purifies hydrogen produced by direct methane pyrolysis.

The state-of-the-art PCC electrolyte, BaZrO<sub>3</sub>-based perovskite has been selected as one of the most promising PCC material with chemical stability and high proton conductivity. Detrimental properties of electrolyte for high performance and long-term stability are high proton conductivity, low electronic current leakage, gas tightness, chemical stability, mechanical robustness under operational conditions. The challenge is to fabricate electrolyte layers having these properties on the porous metal support, without corroding the metal support. Physical Vapor Deposition (PVD) is a promising technique that can grow crystalline thin films of multi elemental phases of our study at moderate temperatures and in good crystallinity. In our procedure, ceramic multilayers are implemented on the porous MS combining wet chemical processes below 1000°C for the porous electrode layers and dry PVD techniques below 800 °C for the gas-tight electrolyte coating, which aims to avoid metal corrosion during the processing and to fabricate thin and dense PCC electrolyte of high performance in an effective route. Different PVD technologies, namely Pulsed Laser Deposition (PLD) and Electron-Beam Physical Vapor Deposition (EB-PVD), are applied for the electrolyte coating process. PLD is known as an advanced technic for thin film deposition suitable for complex materials such as perovskite oxides, that can transfer the chemical composition as in the target and crystallize in good crystallinity. On the other hand, EB-PVD is well developed technique for many materials, which can deposit on very large area. Due to the high running cost, PLD technique remains limited to more fundamental research. Developing MS-PCC using PLD will assure the potential of dry coating techniques, while it will address the way towards industrial manufacturing by investigating the MS-PCC by EB-PVD as more application-oriented technique. Two types of porous metal substrates are investigated: commercial porous metal substrates and metal plates with laser-drilled pores, both of which are made of inexpensive ferritic stainless steel. Potential protection coating on MS is investigated to prevent/ reduce Cr deposition and interdiffusion into the ceramic layers, as well as to eliminate corrosion of the metal. In this paper, half cells by different PVD techniques and on different types of substrates are investigated by Scanning Electron Microscopy (SEM)- and X-ray diffraction and discussed in terms of processing and chemical stabilities. The electrochemical tests on the obtained MS-PCC are reported in another paper of this issue.

## Material

Our strategy of MS architecture is to apply multilayers on the MS, combining wet-chemical processing and PVD techniques all below the critical temperature for MS corrosion in oxidizing atmosphere, i.e. 1000°C. The aim and the issues of the material selection is described in the following and the selected component materials for MS-PCC half cells are listed in Table 1.

### Porous metal support and protection layer

Our first approach in MS architecture has been demonstrated using a commercial porous ferritic steel substrate, ITM (Plansee GmbH, Austria), with all the fabrication procedure below 1000°C (4). The pore size of ITM ranges in 10-30 µm, which is favorable for fuel gas diffusion. As an alternative solution, a new type of porous metal substrate is studied in this work: pore structures on commercial ferritic steel plates, Sanergy® HT (Sandvik, Sweden) and Crofer 22 as an optional material, by applying laser drilling with pore dimensions of 30-50 µm, either periodically distributed round-shaped pores or radially carved slits from the center. The advantages of this type are variable design and pore size, and flexible material choice for metal substrates, with that the porosity, pore distribution and the substrate material can be optimized for cell processing and for operation.

The ferritic stainless steel is promising for its low cost and mechanical stability in the operation, however, when processing in ambient atmosphere at high temperatures even below 1000°C, an apparent drawback of ferritic stainless steel is Cr deposition that causes degradation of the performance. Therefore, it is of high importance to minimize Cr deposition from the metal and/or to eliminate Cr diffusion into FL in the cell processing and during the operation. The perovskite electrode ( $\text{La}_{0.80}\text{Sr}_{0.20}\text{MnO}_{3-\delta}$ ) (LSM) has been employed to reduce the Cr diffusion towards FL, which has been demonstrated in our previous work (4). LSM can also work as an electrode and the layer insertion reduces the pore size down to a several hundred nm. It is still favored for the processing to fabricate FL directly on the MS without LSM layer insertion. It is reported that the metallic Co coating is a good candidate of protection layer, which oxidizes on the surface of the ferritic stainless steel to decrease the oxidation rate of the steel substrate and to reduce Cr evaporation about 90% (5).

### PCC electrolyte and fuel electrode (Functional Layer (FL))

State-of-the-art proton conducting perovskite oxide materials,  $\text{BaZr}_{0.7}\text{Ce}_{0.2}\text{Y}_{0.1}\text{O}_{3-\delta}$  (BZCY721) and  $\text{Ba}_{0.85}\text{Sr}_{0.15}\text{Zr}_{0.7}\text{Ce}_{0.1}\text{Y}_{0.2}\text{O}_{3-\delta}$  (BSZCY151020) are investigated as PCC electrolytes, for their promising properties having both high proton conductivity and chemical stability. Doping with  $\text{Y}^{3+}$  to maintain proton conductivity and being partially substituted with  $\text{Ce}^{4+}$  for high performance, higher thermal expansion coefficient (TEC) for better matching with other components, while higher  $\text{Zr}^{4+}$  content ensures its chemical stability against  $\text{CO}_2$ . BSZCY151020 has been developed especially to enhance thermal expansion coefficient (TEC) that can mitigate the TEC mismatch with other components, while retaining the high proton conductivity and chemical stability (6).

For fuel electrode, conventional cermet electrode of BZCY and NiO is selected. The low oxygen partial pressure in the fuel electrode both in fuel cell and electrolysis operation is advantageous for this choice, compared to the problems of NiO cermet utilization in SOC. Different Zr/Ce ratio (20 to 40 mol% of Ce) is studied to investigate their properties such as chemical stability/compatibility with other components, sinterability, TEC and their electrochemical performance.

The component materials used in this work are listed in Table I. TEC of NiO-BZCY cermet may lie in between those of BZCY ( $9\sim 11 \times 10^{-6} \text{ K}^{-1}$ ) (7,8) and NiO ( $13\sim 14 \times 10^{-6} \text{ K}^{-1}$  @200-900°C) (9).

TABLE I. List of materials of the half-cell components in this work.

Acronym	composition	TEC / $10^{-6} \text{ K}^{-1}$	Functionality
BZCY721	$\text{BaZr}_{0.7}\text{Ce}_{0.2}\text{Y}_{0.1}\text{O}_{3-\delta}$	9.3 (7), 10.2 @650-1000°C (8)	Electrolyte
BSZCY151020	$\text{Ba}_{0.85}\text{Sr}_{0.15}\text{Zr}_{0.7}\text{Ce}_{0.1}\text{Y}_{0.2}\text{O}_{3-\delta}$	$\sim 10$ (6)	Electrolyte
NiO-BZCY	$\text{NiO-BaZr}_{0.9-x}\text{Ce}_x\text{Y}_{0.1}\text{O}_{3-\delta}$ $x=0.2, 0.3, 0.4$		Fuel electrode (FL)
LSM	$(\text{La}_{0.80}\text{Sr}_{0.20})_{0.95}\text{MnO}_{3-\delta}$	12.4 (10)	Cr protection / Electrode
ITM	Ferritic steel (26% Cr)	11.3 @ RT-900 °C	Metal support
Sanergy® HT	Ferritic steel (17.5~18.5% Cr)	12 @ RT-800 °C	Metal support

pore size	thickness / $\mu\text{m}$	Material	Manufacture
nm ↑ μm	~1	BZCY, BSZCY151020	PLD, EB-PVD
	20~40	NiO-BZCY	Chem.process
	1~10	Co, LSM, $\text{CeO}_2$ ...	Chem. Process /Oxidation
	300-500	Stainless steel	Commercial

Figure 1. MS-PCC architecture in this work.

## Experimental

### MS architecture

The MS-PCC cell architecture of this work is schematically illustrated in Fig.1. Porous ferritic stainless-steel substrates with thickness of 300~500  $\mu\text{m}$  ensure the cell robustness for PCC. The pore size around 30  $\mu\text{m}$  is reduced down to the nm range by the multilayers with graded pore structure maintaining the pore size and the roughness on the surface for PVD process to fabricate thin, homogeneous and gas-tight electrolyte layer in a thickness of 1  $\mu\text{m}$ . Target thickness is 1  $\mu\text{m}$ , which is presumably better to mitigate residual stress and to minimize ohmic loss of the electrolyte layer. In our previous work using PLD technique for the electrolyte layer processing, the surface morphology was found to be one of the key properties of the substrate that promoted crystallization and increased the crystallinity of the electrolyte (4). As reported in the previous work, intermediate layer of electrolyte phase before PVD coating could improve the surface morphology. Influence of the intermediate layer was also tested. In this work, the metal substrate of about 5×5 cm size had perforate-cut prior to cell processing that can be easily divided into button sized cells of 20~25 mm in

diameter after the development.

### Protection layer and Functional layer

Sanergy® HT has Ce-Co multilayer nano coating. The metal oxide layer formation was investigated by annealing the metal specimen in air at different temperatures for 36 h. LSM layer was fabricated by a lamination or a dip-coating technique, as a ceramic protection coating and as the first pore reducing layer. On the LSM layer, FL of NiO-BZCY was fabricated either by lamination or screen-printing technique. LSM ( $(\text{La}_{0.8}\text{Sr}_{0.2})_{0.95}\text{MnO}_{3-\delta}$ , Fuelcellmaterials, US), NiO (Nickel Oxide Type F, Lomberg GmbH), BZCY721 (Kceracell, South Korea) and BZCY541 (Marion Technologies, France) powders were used to prepare the slurries. For LSM layer, the powder was milled in a methyl-ethyl-ketone/ethanol mixture to prepare a suspension, and then was mixed with PVB (polyvinyl butyral, Sigma-Aldrich, Germany) as a binder and PEG (polyethylene glycol, Sigma-Aldrich, Germany) as a dispersing agent to form a slurry. For laminated NiO-BZCY, the same procedure was applied to obtain NiO-BZCY slurries, while for the screen-printed FL, NiO and BZCY powders were mixed with terpineol, containing 3 wt% ethyl cellulose as the binder, on a three-roll mill to form a homogenous ink. For the laminated FL, the obtained homogeneous LSM and NiO-BZCY slurry were cast with a doctor blade into a green tape with a thickness of 10-25  $\mu\text{m}$  separately. The green tapes of LSM and NiO-BZCY were co-laminated onto the substrate under a uni-axial pressure and then calcined at 950 °C for 30 minutes in air. For the screen-printed FL, the LSM ink was dip-coated on the porous metal support and calcined at 950 °C for 10 min in air, then the NiO-BZCY ink was screen printed on top of the LSM layer and calcined at 950 °C for 10 min in air.

### PVD coating

After the FL process, the electrolyte layer was deposited by PLD or EB-PVD techniques. By both coating techniques, electrolyte thickness was targeted at about 1  $\mu\text{m}$ .

PLD. Ceramic pellets of BZCY721 and BSZCY151020 were used as PLD targets. Commercial powder was used for BZCY721 (Kceracell, South Korea), while BSZCY151020 was synthesized by conventional Solid-State Reaction (SSR). The detail of this powder process is described in the previous paper (6). The powders were pressed into pellets and sintered, protecting with sacrificing Ba-compound powder to prevent Ba loss in the pellet. The experimental setup of PLD deposition has been described in detail in earlier work (11). BZCY721 and BSZCY151020 thin films were deposited using a PLD workstation (SURFACE systems + technology GmbH & Co. KG, Germany, with a COMPex Pro 205, Coherent, KrF excimer laser, wavelength of 248 nm and pulse length of 25 ns). Prior to deposition, the chamber was evacuated to basis pressure ( $10^{-6}$  mbar). MS sample was cut into the same size of the PLD sample holder, which could be set without any attachment and could be efficiently heated by the substrate heater. The substrate was heated to 700 °C at a ramp rate of 2 °C  $\text{min}^{-1}$  and  $\text{O}_2$  partial pressures for both heating and cooling steps were  $6 \times 10^{-3}$  mbar. The energy density was set to 1.2  $\text{J cm}^{-2}$ , with laser repetition rate of 3 Hz and target-substrate distance at 6 cm. These PLD conditions were optimized in the previous work to achieve the deposited layers in good crystallinity and to mitigate the risk of delamination.

EB-PVD. The BZCY721 evaporation material in form of sub-mm grains was extracted from a funnel by a rotating, water-cooled copper plate and fed into the electron beam. As the material is continuously transferred and completely evaporated in the hot zone, no composition gradient occurs in the films. The growth rate can be adjusted by the rotation speed of the copper plate and is controlled by a quartz crystal monitor. Typical deposition rates are 20 nm/min. MS substrates are heated to the temperature for deposition and rotated with 5 Hz during deposition. The rotation in combination with the large distance between evaporation zone and substrate leads to very homogeneous coatings with thickness variation of less than  $\pm 5\%$  over the full deposition area. The heater features an oxidation zone, where an oxygen pressure of  $5 \times 10^{-3}$  mbar can be reached, enough to fully oxidize the coating. After deposition the films are cooled down in pure oxygen atmosphere. The deposition temperature was optimized by comparing the coated samples on MgO(100) substrate. Considering the crystallinity, stability and grain size of the coating, the deposition temperature was determined as 725°C.

#### Half-cell structural analyses

Zeiss ULTRA PLUS (Carl Zeiss AG, Germany) was used for SEM observation in combination with a Bruker XFlash 5010 energy-dispersive X-ray spectroscopy (EDX) detector for elemental analysis and elemental mapping investigation of the samples. Material phases of the samples were analyzed by X-ray diffraction (XRD) in the Bragg-Brentano geometry using D8 Discover GADDS, equipped with a VÅNTEC-2000 area detector (Bruker AXS, Germany). A tuned monochromatic and collimated Cu-K $\alpha$  line was used.

## **Results and discussion**

#### Protection layer

A SEM cross section and XRD patterns of as-received and air-annealed samples of Sanergy® HT substrate are shown in Fig. 2 and 3. It is suggested by the supplier that Sandvik Sanergy® HT provides a multi-layered Ce-Co nanocoating. EDX mapping revealed that the dark colored layers of about 1  $\mu\text{m}$  thickness at the interface of MS and FL in SEM are corresponding to chromium oxide and Co-Mn phases as indicated in Fig. 2. Main observed phases in XRD are the ferritic steel, Cr<sub>2</sub>O<sub>3</sub> and Co-Mn-O spinels. The as-received specimen shows CoCo<sub>2</sub>O<sub>4</sub> spinel phase while no Co or Ce metal phases were observed. The chemical composition data of Sanergy® HT suggests the substrate contains equal or less than 1% Mn, which might have diffused towards the metal surface to substitute Co in the spinel phase when annealed at high temperatures. The evolution of Co-Mn ratio in the spinel phase is apparent by the identified phase, which was consistent with the EDX analysis: Co in the spinel phase in as-received sample was gradually substituted with diffused Mn and increases with temperature to form MnCo<sub>2</sub>O<sub>4</sub> at 960°C. SEM-EDX analysis could not detect the Ce containing layer very clearly, but XRD confirmed the existence of CeO<sub>2</sub> phase when the substrate is annealed above 900°C.

The fact that the Cr<sub>2</sub>O<sub>3</sub> layer is completely covered by the Co-Mn spinel phase demonstrates the spinel phase works as a protective coating for Cr diffusion towards FL. Electric conductivity of the spinel phases of transition metals are reported (12), among

which  $\text{MnCo}_2\text{O}_4$  shows the highest,  $60 \text{ S cm}^{-1}$  at  $800^\circ\text{C}$ , while that of  $\text{CoMn}_2\text{O}_4$  and  $\text{CoCo}_2\text{O}_4$  are  $6.4$  and  $6.7 \text{ S cm}^{-1}$ , respectively, which are still acceptable for such a small thickness.

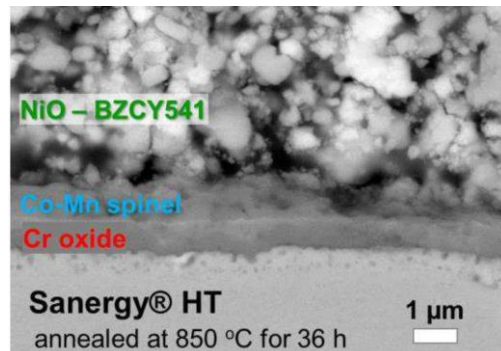


**Figure 2.** SEM cross section of the Sanergy® HT substrate directly coated with the FL, NiO-BZCY541 and annealed at  $850^\circ\text{C}$  for 36 h in air. The phases determined by EDX mapping are indicated in the figure.

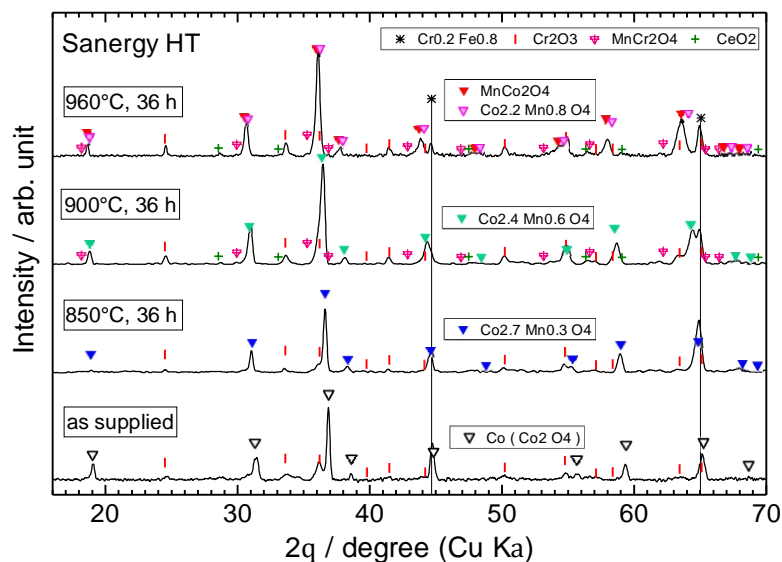


**Figure 3.** XRD patterns of Sanergy® HT metal substrate as-received and annealed at different temperatures for 36 h in air.

### Half cells

With optimized fabrication procedures, crack-free smooth electrolyte coatings were obtained on both porous metal substrates. SEM cross sections of the half cells are displayed in Fig. 4. In both half cells, gradual pore size reduction from LSM to FL is clearly observed that enabled the gas tight electrolyte layer deposition of  $1 \mu\text{m}$  thickness by PLD and EB-PVD. The multilayer structure is also promising to reduce the roughness of the MS to achieve a very smooth surface morphology in the electrolyte layer. It should be noted here that the FL in these cells were fabricated by different methods; the left and the right cells were processed by laminate and screen print methods, respectively. Apparent differences



are thickness and pore size. The left cell presents finer pore sizes than that of the right one, which comes from the particle size difference of the slurries used for the laminate and the screen print methods, rather than their methodological differences. Therefore, the pore size can be controlled by the particle size in the slurry. On the other hand, the difference in thickness may be due to the difference of the methods. The combination of laminate method with PLD coating technique ensures the high quality of the ceramic layers, while that of screen print method with EB-PVD coating technique offers scalable and cost-effective route for more practical applications.

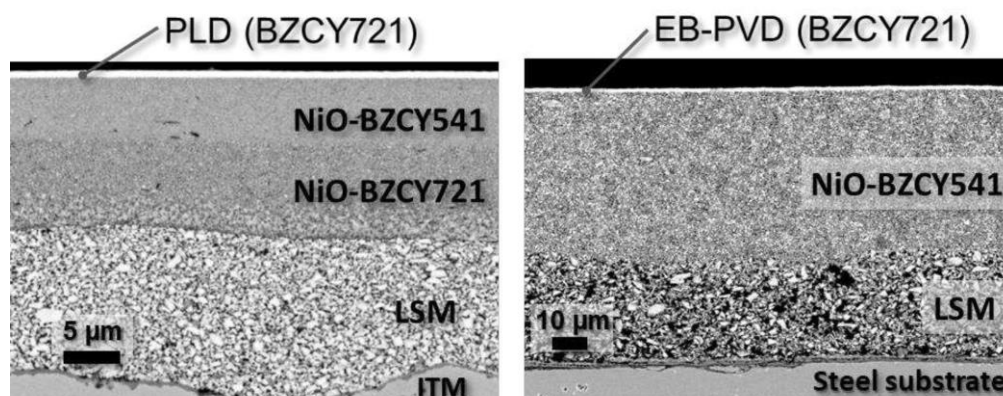


**Figure 4.** SEM cross sections of the MS-PCC with thin film electrolyte of BZCY721 coated by PLD (left) and EB-PVD (right) techniques. The FLs were fabricated by laminate method and screen print method for the cells on the left and the right, respectively.

Small amount of Mn and Cr was found by EDX in the FL on ITM substrate, which might have diffused through the porous LSM layer. By an EDX line scan, it was observed the Cr diffused up to the brighter contrast area at the lower part of NiO-BZCY721 layer. Although LSM could slow down the Cr diffusion, the LSM remains incomplete for Cr protection since the LSM should be porous for the gas diffusion. It is also important to avoid Cr deposition onto the other side of the cell during processing. Therefore, the dense protection coating on the metal substrate such as Co is indispensable to avoid Cr diffusion. The observed Mn in the FL was found to be in  $\text{BaMnO}_4$  phase in XRD pattern (Fig. 5). This impurity phase was more pronounced in the NiO-BZCY541 than that in NiO-BZCY721 when it was fine particle in the slurry, which reaction may be accelerated with higher Ce ratio. The double layer structure of FL with NiO-BZCY721 and NiO-BZCY541 could not only mitigate the reacted phase of  $\text{BaMnO}_4$ , but also enable gradual pore size reduction towards the surface as shown in the SEM, presumably because of the higher sinterability of BZCY541. No  $\text{BaMnO}_4$  peak was observed in this double layer due to larger thickness of FL Fig. 5, which does not assure the absence of the reaction.

By comparing the XRD patterns of the FL on the same substrates in Fig. 5 and 6, the diffraction peaks of the electrolyte layers are well distinguished for both types of the half cells. Both BZCY721 and BSZCY151020 phases are observed as in their powder patterns, suggesting polycrystalline perovskite layers of randomly orientated crystalline grains. It is noticed, however, that the electrolyte diffraction peaks are sharper in the PLD coated samples compared to those of EB-PVD. This indicates higher crystallinity in the PLD coated layers than those in the EB-PVD coated ones. Furthermore, the perovskite peaks in

EB-PVD coated layers using BZCY721 powder as feed material are at remarkably lower angles as indicated with the blue arrow in Fig. 6. It was clarified by the chemical composition analysis of the layer that the sputtering rate of Zr was remarkably lower than that of Ce in the case of EB-PVD, which caused the reduction of Zr ratio in BZCY, i.e. the phase shift towards Ce rich composition. To overcome this lower sputtering rate of Zr, YSZ or ZrO<sub>2</sub> powder was added to the feed material. As indicated in Fig. 6, the perovskite peaks shift with added YSZ or ZrO<sub>2</sub>, which corresponds to the phase change to Zr rich phases, while no Zr fluorite phase or no other secondary phase was observed. This approach successfully demonstrated that the Zr/Ce ratio in the perovskite phase could be adjusted by adding Zr source in EB-PVD coating.

The gas tightness of the half cells was assessed by an air leak rate measurement at room temperature. A few samples showed apparent leakage, however, most of the developed half cells in optimized FL and PVD conditions had a leak rate in the range from 10<sup>-3</sup> down to 10<sup>-4</sup> Pa m<sup>3</sup> s<sup>-1</sup> cm<sup>-2</sup>, among which the best value of 3.16×10<sup>-4</sup> Pa m<sup>3</sup> s<sup>-1</sup> cm<sup>-2</sup> was obtained. The best gas leak rate meets the requirements of the quality control threshold below 5×10<sup>-4</sup> Pa m<sup>3</sup> s<sup>-1</sup> cm<sup>-2</sup>, and is close to the value of 0.7~1.2×10<sup>-4</sup> Pa m<sup>3</sup> s<sup>-1</sup> cm<sup>-2</sup> reported for metal supported solid oxide cells with PVD thin film electrolytes (13). The developed cell was tested at elevated temperatures under H<sub>2</sub> and air flow to NiO-BZCY and counter electrodes, respectively. The tested thin film electrolyte did not show macroscopic signs of spalling or delamination and further investigations at a microscopic scale are on-going.

## Conclusion

The pre-coated Co layer on the stainless-steel substrate was approved to form Co-Mn spinel layer by reacting with Mn from the substrate when annealed at 850 – 960°C in air which can protect Cr<sub>2</sub>O<sub>3</sub> to the functional layer that causes degradation of the cell performance. By gradually reducing the pore size of the metal support from ~30 μm to nm range on the functional layer surface using wet-chemical processing methods, thin and dense electrolyte layers of BZCY721 and BSZCY151020 of 1 μm thickness were successfully deposited on porous metal supports by PLD and EB-PVD techniques, of which half cells could demonstrate very low gas leak rate down to 3.16×10<sup>-4</sup> Pa m<sup>3</sup> s<sup>-1</sup> cm<sup>-2</sup>. The adhesion and chemical stability of the functional layer having smooth surface are essential to achieve a dense and stable electrolyte layer, while an appropriate PVD condition, such as substrate temperature, deposition rate, target material, is detrimental to grow the electrolyte layer of high crystallinity. The chemical composition of the electrolyte layer was correspondent to the target perovskite phase when coated by PLD. On the other hand, sputtering rate of Zr was remarkably lower than that of Ce, causing compositional shift in the coated layers by EB-PVD. By increasing Zr content with additional YSZ or ZrO<sub>2</sub> in the feed material, it was demonstrated that the Zr/Ce ratio could be adjusted to achieve a target composition, which is promising to apply the cost-effective EB-PVD technique to MS-PCC manufacture process.

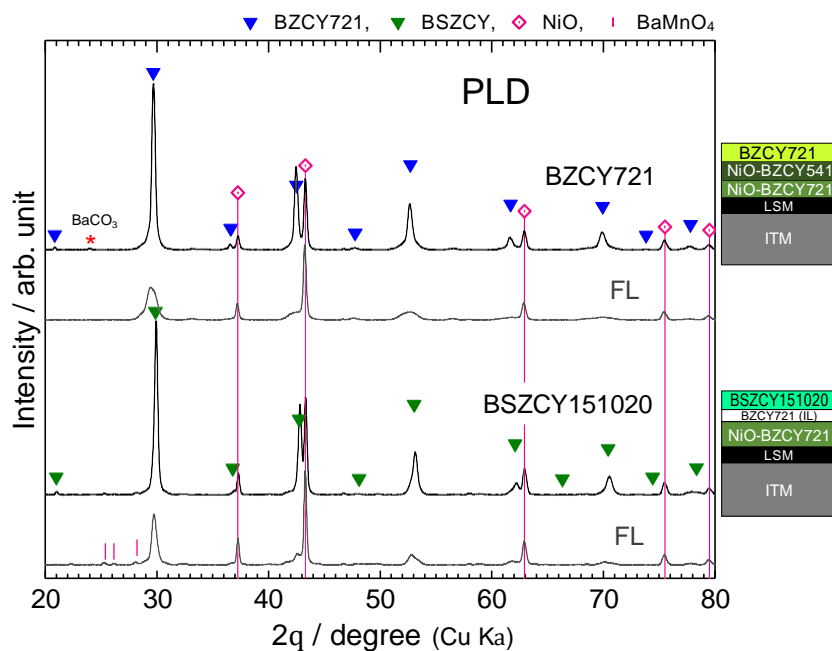


**Figure 5.** XRD patterns of the half cells with thin film electrolytes of BSZCY151020 and BZCY721 coated on ITM at 700°C by PLD. The FL for BSZCY151020 and BZCY721 was NiO-BZCY721 and double layer of NiO-BZCY541/NiO-BZCY721, respectively, fabricated by laminate method.

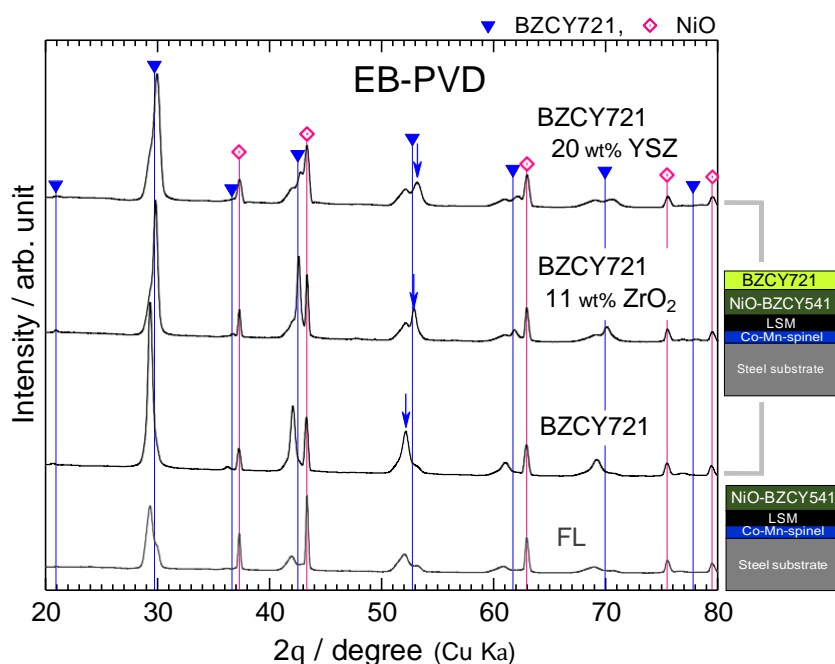


**Figure 6.** XRD patterns of the half cells with thin film electrolyte of BZCY721 coated on Sanergy® HT at 725°C by EB-PVD. The FL of NiO-BZCY541 was fabricated by screen print method. The blue arrows indicate a diffraction peak of perovskite phase near 53°. It demonstrates the perovskite peaks shifts towards higher angle with added Zr source, YSZ or ZrO<sub>2</sub>, in the feed material.

## Acknowledgments

This work is supported by project DAICHI (EIG CONCERT-Japan, BMBF, 01DR18002), project AH2A (the Research Council of Norway, 268010/E20), project ARCADE (BMBF, 03SF0580A) and project 112CO2 (Horizon2020, 952219). The China Scholarship Council is acknowledged for the Ph.D. fellowship of Haoyu Zheng (201806160173).

## References

1. M. C. Tucker, *J. Power Sources*, 195, 4570 (2010).
2. M. C. Tucker, *International Journal of Hydrogen Energy*, 45, 24203 (2020).
3. D. Udomsilp, J. Rechberger, R. Neubauer, C. Bischof, F. Thaler, W. Schafbauer, N. H. Menzler, L. G. J. de Haat, A. Nenning, A. K. Opitz, O. Guillon, and M. Bram, *Cell Reports Physical Science*, 1, 100072 (2020).
4. F. Han, X. Zhou, A. M. Dayaghi, T. Norby, M. Stange, N. Sata, R. Costa, *ECS Transactions*, 91(1), 1035 (2019).
5. J.G. Grolig, J. Froitzheim, and J.-E. Svensson, *J. Power Sources*, 248, 1007 (2014)
6. A. M. Dayaghi, R. Haugrud, M. Stange, Y. Larring, R. Strandbakke, and T. Norby, *Solid State Ionics*, 359, 115534 (2021).
7. A. Løken, S. Ricote, and S. Wachowski, *Crystals*, 8, 365 (2018).
8. G. Hudish, A. Manerbino, W.G. Coors, S. Ricote, *J.Am.Ceram.Soc.*, 101, 1298 (2018).
9. T. H. Nielsen and M. H. Leipold, *J. Am. Ceram. Soc.*, 48, 164 (1965).
10. F. Tietz, *Ionics*, 5, 129 (1999).
11. E. Stefan, M. Stange, C. Denonville Y. Larring, N. Hildenbrand, T. Norby, and R. Haugrud, *J. Materials Science*, 52, 6486 (2017).
12. A. Petric and H. Ling, *J. Am. Ceram. Soc.*, 90, 1515 (2007).
13. R. Costa, F. Han, P. Szabo, V. Yurkiv, R. Semerad, S. K. Cheah, L. Dessemond, *FUEL CELLS*, 18(3), 251 (2018).